JOURNAL OF VIROLOGY, Oct. 1997, p. 7145–7156 Vol. 71, No. 10
0022-538X/97/$04.00+0

Requirements for Different Components of the Host Cell Cytoskeleton Distinguish Ecotropic Murine Leukemia Virus Entry via Endocytosis from Entry via Surface Fusion

KRISHNAKUMAR KIZHATIL AND LORRAINE M. ALBRITTON*

Department of Microbiology and Immunology, College of Medicine, University of Tennessee—Memphis, Memphis, Tennessee 38163

Received 21 November 1996/Accepted 30 June 1997

Murine ecotropic leukemia viruses use a common receptor for entry into host cells; however, the site of virus fusion appears to differ with the host cell. Entry in mouse NIH 3T3 fibroblasts is by endocytosis, whereas entry in rat XC sarcoma cells is by surface fusion. We report here the identification of a step common to both entry pathways, as well as of a step unique to the endocytic pathway. Recent demonstration of the clustering of the virus receptor on rat cells suggested a possible interaction of the receptor with the cellular cytoskeleton (M. H. Woodard, W. A. Dunn, R. O. Laine, M. Malandro, R. McMahon, O. Simell, E. R. Block, and M. S. Kilberg, Am. J. Physiol. 266:E817–E824, 1994). We tested the hypothesis that such an interaction might influence receptor function. We found that entry into NIH 3T3 and XC cells was greatly diminished by the disruption of the actin network before but not shortly after virus internalization, suggesting the actin network plays a critical role in an early step common to both entry pathways. Disruption of microtubules before and shortly after virus internalization markedly reduced entry in NIH 3T3 cells, while entry into XC cells remained efficient. These data suggest that intact microtubules are required in a postpenetration step unique to efficient virus entry via endocytosis. The physiological function of the receptor was not affected by disruption of either the actin network or the microtubules, as the uptake of cationic amino acids in NIH 3T3 and XC cells was comparable to that in control cells even when the cytoskeleton remained disrupted for as long as 3 h.

Viruses initiate infection by binding to the host cell surface. Penetration then occurs by a specific pathway involving either fusion with the plasma membrane at the cell surface or fusion with vesicle membranes after receptor-mediated endocytosis. Among the retroviruses, human immunodeficiency virus (25, 27, 28, 48), avian leukosis virus subgroup A (14), and amphotropic murine leukemia virus (28) appear to fuse at the cell surface, while mouse mammary tumor virus appears to fuse with endocytic vesicle membranes (37). The pathway the ecotropic murine leukemia viruses use is less certain.

In newly infected mouse cells, ecotropic virus particles were seen both inside endocytic vesicles (40) and at the surface undergoing uncoating (31), although it is not clear if one or both observations represent productive virus infection because the particle to infectious unit ratio is very high (38, 39). Additional disparate results revealing the complexity of ecotropic virus penetration emerged from studies of the effects of pH on ecotropic virus entry. They suggest that the mechanism of virus internalization varies with the host cell. Infection of mouse NIH 3T3, SC-1, normal rat kidney, and Rat-1 cells was shown to be sensitive to inhibitors that buffer lysosomal pH, suggesting that fusion occurs in low-pH vesicles after receptor-mediated endocytosis (28). For viruses that use this endocytic pathway, exposure to acidic pH triggers irreversible conformation changes in the envelope protein. This change activates the protein's fusogenic capability, resulting in virus that induce rapid, extensive cell-cell fusion (37, 55). Thus, exposure of NIH 3T3 cells to ecotropic virus at low pH should result in cell-cell fusion. However, it does not (28). Instead, ecotropic virus induce extensive fusion of rat XC sarcoma cells at neutral pH (23, 59). Furthermore, infection of XC cells was found to be insensitive to the lysosomal inhibitors. These data suggested virus internalization occurs by cell surface fusion in this host cell (28). It has been postulated that the differences between the route of internalization in NIH 3T3 and XC cells are determined by characteristics unique to the target cells (28, 56).

We are seeking to determine which, if any, components of the host cell influence the route of virus internalization and penetration. One striking difference between XC cells and NIH 3T3 cells is that XC cells have been highly transformed by activated *src*. Transformation alters the morphology of cells via changes in the cytoskeleton, particularly in the organization of the microtubules and actin network (2, 6, 16, 18). These host cell cytoskeletal components have been found to be involved in early events during infection by viruses from several families. An intact actin network is required for efficient entry of herpes simplex virus type 1 (44) and porcine reproductive and respiratory syndrome virus (24), while nuclear polyhedrosis virus associates with the ends of actin cables as it enters the cytoplasm from endocytic vesicles (8). Simian virus 40 entry does not require the actin network, but its penetration does require intact microtubules (47).

To determine if the cytoskeleton influences ecotropic virus penetration, we examined virus infection in host cells treated with cytochalasin D, a drug that causes rapid depolymerization of the actin network (29, 30), or with nocodazole, a drug that induces rapid depolymerization of microtubules (10). Efficient ecotropic entry into NIH 3T3 and XC cells required an intact actin network. In both cell lines, virus infection was inhibited by cytochalasin D treatment prior to and during virus exposure. However, within 20 min after virus clearance of the cell surface, the actin network was no longer required, suggesting

* Corresponding author. Mailing address: Department of Microbiology & Immunology, College of Medicine, University of Tennessee—Memphis, 858 Madison Ave., Memphis, TN 38163. Phone: (901) 448-5521. Fax: (901) 448-8462. E-mail: lalbritton@UTMEM1.UTMEM.edu.

that an intact actin network is critical to a very early event common to entry into both host cells. Efficient virus entry into NIH 3T3 cells required intact microtubules, while entry into XC cells did not. In NIH 3T3 cells, nocodazole treatment prior to and during virus exposure inhibited infection. In contrast, infection of XC cells was not significantly affected by depolymerization of the microtubules. Virus entry was also inhibited by nocodazole treatment of NIH 3T3 cells 20 min after virus clearance of the cell surface, suggesting that microtubules play a critical role in a postpenetration step in NIH 3T3 cells but not in XC cells.

MATERIALS AND METHODS

Cell lines and virus. Mouse NIH 3T3 fibroblasts were cultured in Dulbecco's modified Eagle's medium (DMEM; GIBCO) supplemented with 8% donor calf serum (GIBCO). XC rat sarcoma cells (ATCC CCL-165) were maintained in DMEM supplemented with 8% fetal bovine serum (GIBCO) and 3.5 mg of D-glucose per ml. The cell line producing replication-defective ecotropic-pseudotyped ψ-2 BAG murine leukemia virus (50), encoding the *Escherichia coli* β-galactosidase gene, was maintained in DMEM supplemented with 8% fetal bovine serum. Polybrene (20 μg/ml; Sigma) was added to all virus stocks prior to exposure to cells.

Cytoskeletal inhibitors and antibodies. Nocodazole {methyl[5-(2-thienylcarbonyl)-1*H*-benzimidazol-2yl] carbamate (molecular weight, 301.31); ICN Pharmaceuticals, Inc.} stock solution (10 mM) was prepared by dissolution in dimethyl sulfoxide (DMSO). A 1-mg/ml stock of cytochalasin D (Sigma) was prepared in DMSO. The anti-β-tubulin monoclonal antibody KMX1 (1 mg/ml; Boehringer Mannheim) was the generous gift of Jianxun Li. The goat anti-mouse monoclonal antibody conjugated to fluorescein isothiocyanate (FITC; 1.4 mg/ml) and phalloidin-conjugated tetramethylrhodamine isothiocyanate (TRITC; 50 μg/ml) were obtained from Sigma.

Treatment of cells with cytoskeletal inhibitors. Nocodazole was used at a final concentration of either 33 or 66 μM by dilution of the stock solution in tissue culture medium. Cytochalasin D was used at 1 μg/ml by dilution of the stock in tissue culture medium. To control for possible effects of the DMSO solvent in the treatments with either nocodazole or cytochalasin D, sets of cells were treated with the appropriate concentrations of DMSO (0.33% [vol/vol] or 0.66% [vol/vol] in experiments with 33 or 66 μM nocodazole, respectively; 0.1% [vol/vol] in experiments with cytochalasin D).

Quantitation of virus infection and cell density. Using phase-contrast microscopy, we determined the cell density on the live cultures immediately after plating. One day later, quadruplicate wells of NIH 3T3 and XC cells were used in infection assays with either pretreatment or postinternalization treatment in 1 μg of cytochalasin D per ml, 33 or 66 μM nocodazole, or no additions as described below for the infection assay. In all cases, the inhibitor was removed after less than 3 h by extensive rinsing with fresh medium without drugs. Cells were incubated at 37°C to allow for cell growth and virus replication. Forty-eight hours later, cells were fixed with glutaraldehyde, stained with the chromogenic substrate 5-bromo-4-chloro-3-indolyl-β-D-galactopyranoside (X-Gal; Boehringer Mannheim), and assayed for β-galactosidase activity indicative of infection. The total number of positively stained (blue) cells in each well was scored under a light microscope. Nuclei were then counterstained with 0.16% basic fuchsin (Sigma), and the total number of nuclei per 3.14 mm^2 in three representative 100× fields of each of the quadruplicate samples was determined under a light microscope to quantitate cell density. The final cell density was calculated as the average of the mean number of nuclei/square millimeter ($n = 4$). Relative infection was calculated as (percentage of infected cells in treated wells/percentage of infected cells in untreated wells) × 100, where the percentage infected = (total of infected cells/total cells) × 100. The total number of cells was calculated by multiplying the average cell densities by the total area of a well (201 mm^2). In all cases, the total number of cells in each sample was greater than 9.5×10^4.

Fluorescence microscopy of the actin network. Cells seeded on replicate coverslips at a density of 500 cells/mm^2 were exposed for 3 h at 37°C to medium containing either cytochalasin D (1 μg/ml) or DMSO or to medium with no additions. A parallel set of cells was exposed to cytochalasin D (1 μg/ml) for 3 h at 37°C, then washed extensively with medium, and incubated for an additional 2 h at 37°C in fresh medium without cytochalasin D to allow recovery from the drug treatment. Each set of coverslips was then prepared to assess the integrity of the actin network. NIH 3T3 cells were rinsed twice with phosphate-buffered saline (PBS) (pH 7.4) supplemented with 1 mM calcium chloride and 1 mM magnesium chloride (PBS-Ca-Mg) and then fixed for 7 min at −20°C with acetone. XC cells were rinsed, fixed for 25 min in 10% formalin, and permeabilized in 0.5% Triton X-100 in PBS-Ca-Mg for 5 min. Fixed cells were incubated with 5% goat serum in PBS-Ca-Mg and incubated with a 1:75 dilution of phalloidin-TRITC in PBS-Ca-Mg supplemented with 5% goat serum. Coverslips were mounted on glass slides and images were captured with a Zeiss Axiophot epifluorescence microscope as described below.

Fluorescence microscopy of microtubules. Cells seeded on replicate coverslips at a density of 500 cells/mm^2 were exposed for 3 h at 37°C to medium containing either 66 μM nocodazole or DMSO or to medium with no additions. A parallel set of cells was exposed to 66 μM nocodazole for 3 h at 37°C, then washed extensively with medium, and incubated for an additional 2 h at 37°C in fresh medium without nocodazole to allow recovery from the drug treatment. Using a modification of a procedure developed specifically for determining the proportion of polymerized microtubules present in cells and described by Zhai and Borisy (60), we prepared each set of coverslips to assess the integrity of the microtubules. Briefly, NIH 3T3 cells were rinsed twice with PBS-Ca-Mg and then fixed for 5 min at room temperature with 1% paraformaldehyde dissolved in 10 mM 1,4-piperazine diethylsulfonic acid (PIPES; pH 6.8)–5 mM EGTA–2 mM $MgCl_2$. XC cells were rinsed as described above but fixed in 10% formalin for 25 min. After a brief rinse with PBS-Ca-Mg, the cells were incubated for 1 min in microtubule-stabilizing buffer (MSB; 100 mM PIPES [pH 6.9], 1 mM EGTA, 2.5 mM GTP, 4% polyethyleneglycol 8000 [7]), a buffer that stabilizes polymerized tubulin but not monomeric tubulin against Triton X-100 treatment. The cells were then extracted with 0.5% Triton X-100 in MSB for 8 min to remove any depolymerized tubulin and washed twice with MSB for 2 min. NIH 3T3 cells were fixed further with acetone at −20°C for 7 min and rehydrated with 5% goat serum in PBS-Ca-Mg. Fixed XC and NIH 3T3 cells were blocked with 5% goat serum in PBS-Ca-Mg, incubated with a 1:50 dilution of mouse antitubulin monoclonal antibody, and then incubated with a 1:250 dilution of goat anti-mouse FITC-conjugated antibody. Coverslips were mounted on glass slides and viewed with a Zeiss Axiophot epifluorescence microscope. Images were captured with a 35-mm camera on 400 ASA Kodak color film.

Virus inactivation. ψ-2 BAG virus was incubated with cells for 30 min at 4°C to allow virus binding but not virus internalization; medium was replaced with pH 3.0 citrate buffer (40 mM sodium citrate, 10 mM KCl, 135 mM NaCl) for 1 min at room temperature. Cells were then rinsed twice with PBS (pH 7.6) to neutralize, and fresh medium was added. Forty-eight hours later, cells were fixed and stained with X-Gal for β-galactosidase activity indicative of infection and with basic fuchsin to stain nuclei. The total number of positively stained (blue) cells as well as the total number of nuclei in each well was then scored under a light microscope. Control cells were treated as described above except that the 1-min incubation with pH 3.0 citrate buffer was omitted.

Infection assays in cells pretreated with cytoskeletal inhibitors. Approximately 2×10^4 cells were plated in each well of a 24-well tissue culture dish (initial cell density of 100 cells/mm^2). Quadruplicate wells were exposed to 33 or 66 μM nocodazole, DMSO, or medium containing no additions for 45 min at 37°C to depolymerize the microtubules. Cells were then incubated with ecotropic-pseudotyped ψ-2 BAG virus in the presence of 33 or 66 μM nocodazole for virus applied to cells pretreated with nocodazole (to maintain disruption of the microtubules during infection) and in the presence of DMSO or no additions for virus applied to control cells. After 2 h of exposure, cells were treated with citrate buffer (pH 3) to inactivate any virus that had not penetrated the cells. The cells were then washed twice with PBS, washed four times with fresh medium to neutralize and to remove nocodazole and DMSO, and then fed with fresh medium. Forty-eight hours later, cells were fixed and stained as described above for β-galactosidase activity indicative of virus infection. The total number of positively stained (blue) cells in each well was then scored by phase-contrast microscopy. Infection assays were performed as above to quantitate the effect of disruption of the actin network on virus infection by using cytochalasin D (1 μg/ml) instead of nocodazole.

Postinternalization assay. Cells cultured in a 24-well tissue culture plate were chilled on ice and then exposed to ecotropic ψ-2 BAG virus at 4°C to allow binding of the virus to the cells but not penetration of the host cell membrane. After 30 min of binding, the plate was transferred to a 37°C water bath for 20 min to allow virus internalization. Cells were incubated with citrate buffer (pH 3) to inactivate any virus that had not penetrated the host cells and were washed twice with PBS to neutralize and four more times with fresh medium. Medium containing either 66 μM nocodazole or 1 μg of cytochalasin D per ml was added to quadruplicate wells. After 3 h of incubation at 37°C, cells were rinsed three times with PBS and five times with fresh medium to remove drugs and allow recovery of the cytoskeleton. Two days later, cells were fixed and stained for β-galactosidase activity indicative of productive infection. This procedure was performed in parallel on control cells, using DMSO or no additions instead of nocodazole or cytochalasin D.

Cationic amino acid transport assay. The cationic amino acid uptake assay was performed by a modification of the arginine transport assay as previously described (51). Briefly, 12 wells of a 24-well tissue culture plate were seeded with 2.5×10^4 NIH 3T3 cells. When the cell monolayers reached 80% confluence (typically after 50 h), quadruplicate wells were exposed to 66 μM nocodazole for 45 min, 2 h, or 3 h at 37°C to disrupt the microtubules. During the last 20 min of each incubation time, intracellular pools of amino acid were reduced while maintaining the inhibitor as follows. Cells were washed with amino acid-free Earle's balanced salt solution (EBSS; 1.8 mM $CaCl_2$, 5.3 mM KCl, 0.8 mM $MgSO_4$, 117 mM NaCl, 1 mM NaH_2PO_4, 5.6 mM glucose) and incubated with 66 μM nocodazole in amino acid-free EBSS at 37°C. Cationic amino acid uptake was initiated by incubating the cells with 66 μM nocodazole in arginine uptake solution (1.25 μCi/ml of L-[^{14}C]arginine and 1 mM unlabeled L-arginine in EBSS) for 2 min at 37°C. Cells were then washed and lysed in 200 μl of lysis

buffer (0.1% sodium dodecyl sulfate, 150 mM NaCl, 10 mM Tris-HCl [pH 7.5], 1 mm EDTA). Protein was precipitated from the lysates by adding trichloroacetic acid (final concentration, 5% [vol/vol]), and the protein concentration was determined by the Bradford protein assay (Bio-Rad). Cytoscint (ICN) was added to the amino acid-containing supernatant resulting from the trichloroacetic acid extraction of the lysates, and the samples were counted in a scintillation counter to quantitate total uptake of L-arginine. The total amino acid uptake by each cell sample was standardized to its protein concentration. Uptake was also assessed for quadruplicate wells of control cells incubated with 0.66% (vol/vol) DMSO or with no drugs instead of nocodazole. Transport assays were performed to quantitate L-arginine transport in cells with disrupted actin networks, using the same protocol except that cytochalasin D (1 μg/ml) was used instead of nocodazole. Additional assays measuring uptake of the cationic amino acid L-lysine were performed as described above except that 33 μM nocodazole or 1 μg of cytochalasin D per ml was used as the cytoskeletal inhibitor for a 45-min incubation period. In these assays, the uptake solution contained 0.5 μCi of L-[^{14}C]lysine per ml and 1 mM unlabeled L-lysine in EBSS.

RESULTS

We began examining the possible involvement of the host cytoskeleton by characterizing ecotropic virus entry in different host cells. We used (i) mouse NIH 3T3 cells as the prototype host cell in which ecotropic virus entry exhibits sensitivity to lysosomal inhibitors but not low-pH-induced cell-cell fusion and (ii) rat XC cells as the host cell in which entry is resistant to lysosomal inhibitors. We disrupted the cytoskeleton with the inhibitors cytochalasin D, a specific inhibitor of actin polymerization, and nocodazole, a specific inhibitor of tubulin polymerization into microtubules (10, 29, 30). Depolymerization of the cytoskeleton by using these inhibitors results in gross morphologic changes in adherent cells: rounding up of cells in the presence of nocodazole and "arborization" of cells treated with cytochalasin D (10, 29, 30). Using phase-contrast microscopy, we observed that NIH 3T3 and XC cells treated with 33 or 66 μM nocodazole rounded up, and those treated with 1 μg of cytochalasin D per ml arborized within 45 min after exposure. Cells incubated with the inhibitors for longer than 3 h began detaching from the culture plates. To avoid cell losses due to detachment, the total time of drug exposure in infection and transport assays was kept to less than 3 h. In addition, cultures were observed by light microscopy before exposure and again immediately after drug removal to monitor for cell detachment.

Removal of cytochalasin D after a 3-h exposure allowed the actin network to repolymerize. Ecotropic viruses require at least one cell division to establish a provirus during infection (41). Roe and colleagues have shown that virus will bind and enter cells arrested in the cell cycle but that integration of the provirus does not occur (41). Prolonged actin depolymerization using cytochalasin B, a compound closely related to cytochalasin D, prevents cytokinesis (12, 46). However, Roe and coworkers found that releasing a 10-h block of the host cell cycle allowed virus replication to proceed (41). Thus, our experimental design depended on disrupting the actin network with cytochalasin D and then reversing the disruption by removal of the inhibitor, allowing the cell cycle to continue so that any observed decrease in infection would be caused by a requirement for the actin network in virus entry and not by a downstream block in establishing the provirus. Removal of cytochalasin D after short exposures has been shown to be followed by rapid repolymerization of the actin network in a number of different cell lines (30). However, the reversibility of depolymerization upon removal of cytochalasin D had not been examined in NIH 3T3 and XC cells.

We examined the actin network in cytochalasin D-treated NIH 3T3 and XC cells by direct fluorescence using a phalloidin-rhodamine conjugate that binds avidly to polymerized actin. In marked contrast to the arrays of actin microfilaments seen in untreated cells (Fig. 1A and D), cytochalasin D-treated cells exhibited a diffuse pattern of actin (Fig. 1B and E), indicating the stress fibers and the cortical actin network were depolymerized. We then determined if NIH 3T3 and XC cells would repolymerize their actin networks after drug removal. Cells were treated for 3 h with cytochalasin D (1 μg/ml), washed, and allowed to recover. Direct fluorescence using phalloidin-rhodamine as described above showed that the gross features of the actin network (Fig. 1C and F) were restored within 2 h after removing the inhibitor. Thus, in all experiments, we removed cytochalasin D after the indicated time of total exposure (in no case longer than 3 h of exposure) to allow reorganization of the actin network and cell division.

Inactivation of ecotropic virus by treatment with pH 3.0 citrate buffer. Previous studies by others have shown that ecotropic virus can be readily inactivated by treatment with trypsin. However, alterations of the cytoskeleton caused by cytochalasin D and nocodazole resulted in weak adherence of cells to the culture plates. To avoid extensive host cell detachment during inactivation, we used a modification of a method described to inactivate herpes simplex virus in studies of the effects of cytochalasin D on penetration (44). Rosenthal et al. found that unbound herpesvirus and virus that was bound but not internalized were inactivated by a 1-min exposure to pH 3.0 citrate buffer; internalized virus was not affected by this treatment (43). Ecotropic viruses have been shown to be stable at pH as low as 4.0 (28), but the effects of exposure to pH 3.0 were not studied. We incubated ecotropic-pseudotyped BAG virus with replicate cultures at 4°C for 30 min to allow for virus binding without internalization. Half of the samples were exposed to pH 3.0 citrate buffer for 1 min and then washed with PBS, and fresh medium was added. The remaining samples were washed with PBS alone before addition of fresh medium. All cultures were incubated at 37°C for 48 h and then fixed and stained for assay of β-galactosidase activity transduced by the BAG virus genome. Removal of virus with PBS alone after 30 min binding resulted in infection of 0.140% ± 0.075% of the cells ($n = 6$), whereas exposure of cells and bound virus to the low pH citrate wash resulted in infection of 0.001% ± 0.002% of cells ($n = 6$). These results indicate that 99% of the bound ecotropic virus was inactivated upon exposure at pH 3. The remaining 1% of virus either was resistant to inactivation or may have internalized during the 30-min incubation at 4°C.

Depolymerization of the actin network inhibits virus infection at a step before virus penetration of the host cell plasma membrane in NIH 3T3 and XC cells. NIH 3T3 and XC cells were pretreated with cytochalasin D (1 μg/ml) for 45 min to depolymerize the actin network and then exposed to ecotropic-pseudotyped BAG virus for 2 h. The drug was maintained for the duration of virus exposure. Cells were washed with low-pH citrate buffer to inactivate virus that had not internalized, and fresh medium was added. Forty-eight hours later, cells were fixed and stained to assay for β-galactosidase activity transduced by virus. Both cell types exhibited profound inhibition of virus infection after pretreatment with cytochalasin D. Figure 2 shows the results of the experiments in which 82% inhibition of infection was obtained in pretreated NIH 3T3 cells and 79% inhibition was obtained in pretreated XC cells. Overall infection of NIH 3T3 cells was reduced by an average of 78% in four independent pretreatment experiments, and infection of XC cells was reduced by an average of 72% in three independent experiments (Table 1).

We evaluated the effects of DMSO, the solvent for cytochalasin D, by quantitating infection in cells treated only with 0.1% DMSO. Infection in DMSO-treated cells was slightly higher than that in uninfected cells in all experiments with both

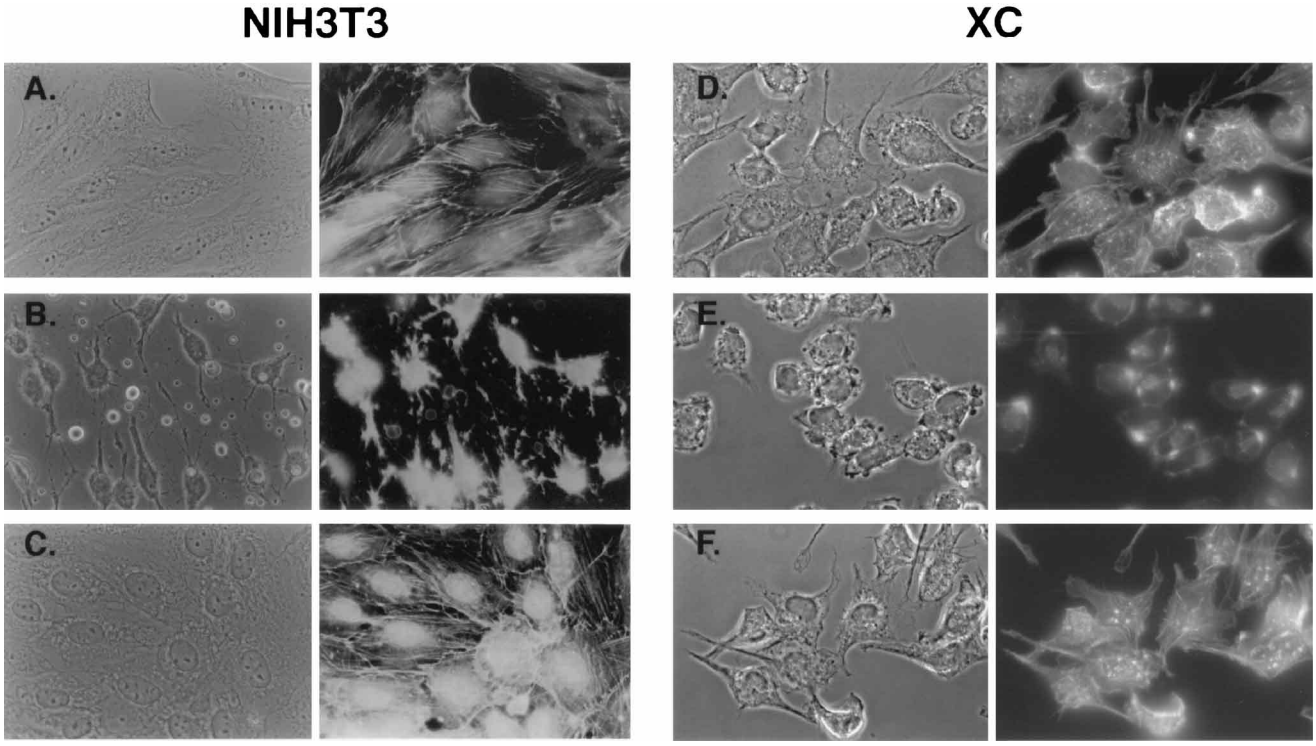

FIG. 1. Recovery of the actin network organization occurs within 2 h after withdrawal of cytochalasin D. NIH 3T3 and XC cells were prepared for fluorescence microscopy as described in Materials and Methods and stained with phalloidin-TRITC to visualize the actin network in untreated cells (A and D), cells treated with cytochalasin D (1 μg/ml) for 3 h (B and E), and cells treated with cytochalasin D (1 μg/ml) for 3 h then allowed to recover after the removal of cytochalasin D for 2 h (C and F). The left panel of each section shows the phase-contrast photomicrograph of the cells viewed by fluorescence microscopy in the right panel.

cell types. NIH 3T3 cells pretreated with DMSO exhibited an average increase in infection of 12% in four independent experiments, and XC cells exhibited an average increase of 7% in three independent experiments (data not shown).

To determine if the involvement of the actin network is critical to an early or to a later step in the virus life cycle, we performed experiments in which the network was not disrupted until after virus binding and internalization had occurred. This postinternalization assay consisted of the following steps. Cells were exposed to virus at 4°C to allow virus binding without internalization to provide a population of cells undergoing near-synchronous virus entry. Cells were then washed with a neutral buffer to remove unbound virus and shifted to 37°C to allow penetration of the plasma membrane. Twenty minutes later, cells were washed with low-pH citrate buffer to inactivate any virus that had not been internalized. The actin network was then depolymerized by adding 1 μg of cytochalasin D per ml to the cell culture medium (disruption of the actin network starts within 2 to 3 min after exposure to this concentration of cytochalasin D [29]). Infection of NIH 3T3 and XC cells treated after virus internalization was comparable to that of untreated cells. Infection of NIH 3T3 cells was an average of 2% less than that of untreated cells in the four independent experiments, and infection of XC cells was equivalent to that of untreated cells in three independent experiments (Table 1). Figure 2 shows the results of the experiments in which a 4% reduction in infection was obtained in postinternalization-treated NIH 3T3 cells and an increase of 1% was obtained in treated XC cells. Infection in DMSO-treated cells was comparable to that in untreated cells. DMSO-treated NIH 3T3 cells exhibited an average increase in infection of 9% in the four experiments, and XC cells exhibited an average increase of 4% in three independent experiments (data not shown).

Having obtained a marked reduction of infection in the pretreatment experiments, we were concerned that the repolymerization of the actin network that we observed upon removal of cytochalasin D might not correlate with release of a block to mitosis in the treated cultures. To determine if the cell cycle was blocked and remained so in treated cultures, we compared the average number of cell divisions in the treated cultures to that in untreated cultures in each infection assay. The cell density at the beginning (at cell plating) and upon termination of each infection experiment was quantitated and used to calculate the average number of cell divisions over the duration of the experiment. Cell division proceeded at comparable rates in cultures pretreated with cytochalasin D and in untreated cultures (Table 2). Untreated NIH 3T3 cultures averaged 3.2 divisions, and cytochalasin D-treated cells averaged 3.1 divisions. Untreated XC cells averaged 3.5 cell divisions, and treated cultures averaged 3.2 divisions. Because the untreated cultures were infected (Table 1), they must have undergone at least one of the three divisions after they were exposed to virus (41). Since all cultures in an experiment were plated by aliquoting a single pool of cells, those treated cultures that averaged the same number of divisions as untreated cells most likely underwent at least one mitosis after exposure to the virus and inhibitors as well. Furthermore, similar numbers of cell divisions were observed for treated cells in the postinternalization experiments (data not shown), where infection of both cell types was not inhibited by a 3-h exposure to cytochalasin D after virus internalization (Table 1). These data suggest that any block to cell division in either NIH 3T3 or XC cells was temporary and was unlikely to have interfered with

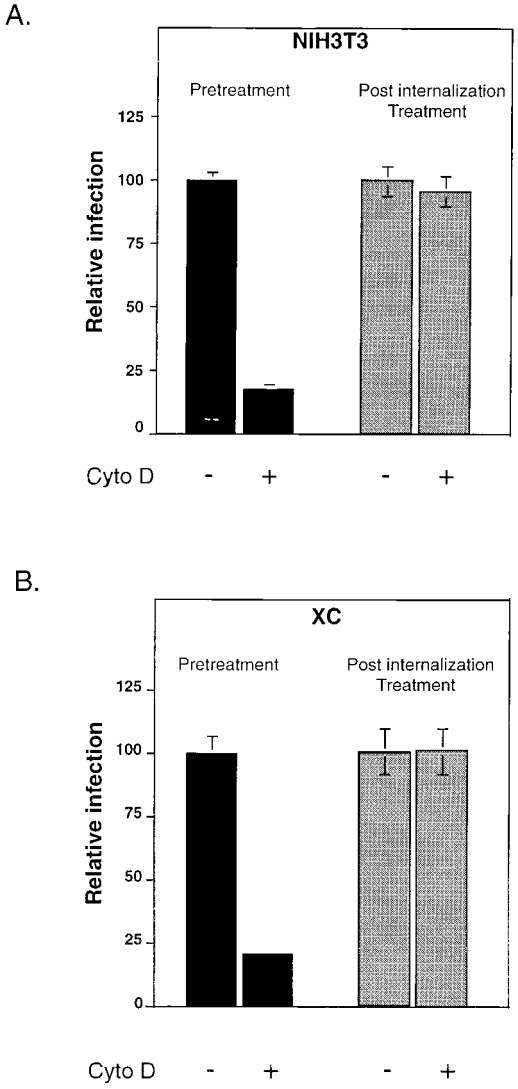

FIG. 2. Depolymerization of the actin network inhibits ecotropic virus infection at a step before internalization of virus in NIH 3T3 cell and XC cells. Pretreatment, cells were treated with cytochalasin (Cyto) D (1 μg/ml) for 45 min then exposed to ψ-2 BAG virus for 2 h. Cytochalasin D was maintained at 1 μg/ml during virus exposure. Post internalization Treatment, cells were treated with cytochalasin D (1 μg/ml) 20 min after virus internalization as described in Materials and Methods. Values shown for infection data from experiment I for both cell types are the means of four samples for each treatment. The error bars represent maximal variation.

virus infection sufficiently to account for the marked decrease in infection observed.

Removal of nocodazole after a 3-h exposure allowed the microtubules to repolymerize. Because microtubules play essential roles in mitosis, prolonged exposure to nocodazole also arrests the cell cycle (61). As with cytochalasin D, the removal of nocodazole after short exposures has been shown to be followed by rapid repolymerization of the microtubules, allowing the cell cycle to progress (10, 15). Again our experimental design depended on reversing the disruption of microtubules by removal of the inhibitor, allowing the cell cycle to continue. The repolymerization of microtubules upon removal of nocodazole had not been examined in NIH 3T3 and XC cells.

To examine the integrity of the microtubules, we performed indirect immunofluorescence with an antitubulin monoclonal antibody, using a modification of a procedure developed specifically for determining the proportion of polymerized microtubules present in cells (60). Briefly, fixed cells were extracted by detergent in the presence of MSB prior to incubation with antitubulin. MSB stabilizes polymerized tubulin against detergent extraction, preventing its removal from extracted cells. Tubulin that is not incorporated into the microtubule polymer is not stabilized and is removed from cells during extraction. Untreated NIH 3T3 and XC cells exhibited abundant strands of intact microtubules that were resistant to detergent extraction (Fig. 3A and D). In contrast, cells treated with nocodazole displayed only low levels of diffuse tubulin, indicating that microtubules had depolymerized, allowing extraction of tubulin prior to incubation with the antibody (Fig. 3B and E). We then determined if NIH 3T3 and XC cells would repolymerize their microtubules after drug removal. Cells were treated for 3 h with 66 μM nocodazole, washed, and allowed to recover. Indirect immunofluorescence using antitubulin as described above showed that the gross features of microtubules (Fig. 3C and F) were restored within 2 h after removing the inhibitor. Thus, in all experiments, we removed nocodazole after the indicated time of total exposure (in no case longer than 3 h of exposure) to allow reorganization of the cytoskeleton and cell division.

Depolymerization of microtubules inhibits virus infection in NIH 3T3 cells but not in XC cells by affecting an event after internalization of virus. NIH 3T3 and XC cells were pretreated to depolymerize the microtubules before and during virus exposure with 33 or 66 μM nocodazole. Compared to untreated cells, NIH 3T3 cells treated with 33 μM nocodazole exhibited a marked reduction in infection. In contrast, infection of nocodazole-treated XC cells was comparable to that of untreated cells. There was an average reduction in infection of nocodazole-treated NIH 3T3 cells of 71% in four independent pretreatment experiments, while infection of treated XC cells was an average of 7% less than in untreated cells (Table 3). Figure 4 shows the results of the experiments in which a 75% inhibition of infection was observed in pretreated NIH 3T3 cells and a 16% reduction in infection was observed in XC cells. Similar results were obtained with 66 μM nocodazole: infection of NIH 3T3 cells was inhibited by 86%, whereas XC cell infection was 2% greater than in untreated cells (Table 3).

Because nocodazole was dissolved in as high as 0.66% DMSO, a concentration much greater than that used in the studies with cytochalasin D, we also quantitated infection in cells pretreated only with 0.33 and 0.66% DMSO. Infection in DMSO-treated cells was comparable to that in uninfected cells in both cell types. NIH 3T3 cells treated with 0.33% DMSO exhibited an average increase in infection of 3% in four independent experiments, and XC cells exhibited an average increase of 7% in three independent experiments (data not shown). Pretreatment with 0.66% DMSO increased infection by 11% in NIH 3T3 cells and by 13% in XC cells (data not shown).

We performed postinternalization assays using nocodazole to determine if an early or a later step in virus entry is affected by disruption of the microtubules. Nocodazole was added to the cell culture medium after a period of 20 min was allowed for virus internalization. Because disruption of microtubules occurs within 10 min after exposure to 3.3 μM nocodazole (10), we tried 33, 66, and 132 μM nocodazole to obtain as rapid a depolymerization as possible for this assay. Cells remained adherent to the culture plate when treated with 33 and 66 μM drug for 3 h but detached when treated with 132 μM. Thus, 66 μM nocodazole was used in these experiments. NIH 3T3 cells treated with nocodazole after virus internalization exhibited a

TABLE 1. Infection in cytochalasin D-treated cells

Cell line	Expt[a]	% Infected cells[b]		Relative infection[c] (%)	Relative inhibition[d] (%)	Avg
		No inhibitor	Cytochalasin D			
NIH 3T3	Pre					
	I	0.130 ± 0.008	0.023 ± 0.005	18	82	
	II	0.142 ± 0.032	0.041 ± 0.009	29	71	
	III	0.119 ± 0.010	0.029 ± 0.003	24	76	78
	IV	0.062 ± 0.004	0.013 ± 0.003	21	79	
	Post					
	I	0.052 ± 0.006	0.050 ± 0.006	96	4	
	II	0.074 ± 0.005	0.069 ± 0.012	93	7	
	III	0.063 ± 0.007	0.059 ± 0.010	94	6	2
	IV	0.056 ± 0.010	0.061 ± 0.012	109	↑ 9	
XC	Pre					
	I	0.129 ± 0.019	0.027 ± 0.002	21	79	
	II	0.186 ± 0.016	0.075 ± 0.001	41	59	72
	III	0.130 ± 0.004	0.027 ± 0.005	21	79	
	Post					
	I	0.093 ± 0.008	0.094 ± 0.016	101	↑ 1	
	II	0.224 ± 0.017	0.252 ± 0.035	113	↑ 13	0
	III	0.060 ± 0.005	0.051 ± 0.003	86	14	

[a] Pre, pretreatment. Cells were exposed to cytochalasin D (1 μg/ml) for 45 min and then exposed to the inhibitor plus ecotropic virus for an additional 2 h as described in Materials and Methods. Post, postinternalization. Cytochalasin D (1 μg/ml) was added to cells 20 min after virus internalization.
[b] (Number of infected cells/total number of cells) × 100. Values shown are the mean of replicate samples ± 1 standard deviation ($n = 4$).
[c] (Percent infected cells in the treated population/percent infected cells in the untreated population) × 100.
[d] Calculated as (100 − relative infection). Values representing an increase in infection are indicated by arrows.

marked reduction in infection, while infection of treated XC cells was comparable that of untreated cells. Infection of NIH 3T3 cells was inhibited by an average of 81% in three independent experiments (Table 3). Figure 4A shows the results of the experiment in which 79% inhibition was observed. In contrast, infection in XC cells was an average of 2% less than in untreated cells (Table 3). Figure 4B shows the results of the experiment in which a 7% reduction was observed. DMSO-treated NIH 3T3 cells exhibited an 11% average increase in infection and XC cells exhibited an average increase of 4% in infection (data not shown).

Here too there was the possibility that the repolymerization of the microtubules that we observed upon removal of nocodazole might not correlate with release of a block to mitosis,

TABLE 2. Effects of cytoskeletal inhibitors on the number of cell divisions

Cell line	Cytochalasin D				Nocodazole			
	Treatment	Final cell density (cells/mm^2)[a]	Avg cell divisions[b]	Expt[c]	Treatment	Final cell density (cells/mm^2)[a]	Avg cell divisions[b]	Expt[c]
NIH 3T3	−	971	3.3	I	33 μM			
	+	855	3.1		−	1,166	3.6	I
	−	942	3.3	II	+	919	3.2	
	+	985	3.3		−	906	3.2	II
	−	924	3.2	III	+	855	3.1	
	+	945	3.3		−	1,054	3.4	III
	−	741	2.9	IV	+	646	2.7	
	+	683	2.8		66 μM			
					−	652	2.7	IV
					+	518	2.4	
XC	−	902	3.2	I	33 μM			
	+	668	2.8		−	902	3.2	I
	−	1,590	4.0	II	+	920	3.2	
	+	1,579	4.0		−	1,590	4.0	II
	−	920	3.2	III	+	478	2.3	
	+	690	2.8		−	920	3.2	III
					+	890	3.2	
					66 μM			
					−	1,441	3.8	IV
					+	1,280	3.7	

[a] Average cell density at the end of each pretreatment experiment calculated as described in Materials and Methods.
[b] The number of cell divisions was calculated as (log D_f − log D_i)/log 2, where D_f is the final cell density and D_i is the initial cell density. The initial density of all cultures was 100 cells/mm^2.
[c] Numbers correspond to pretreatment experiments whose infection data are listed in Tables 1 and 3.

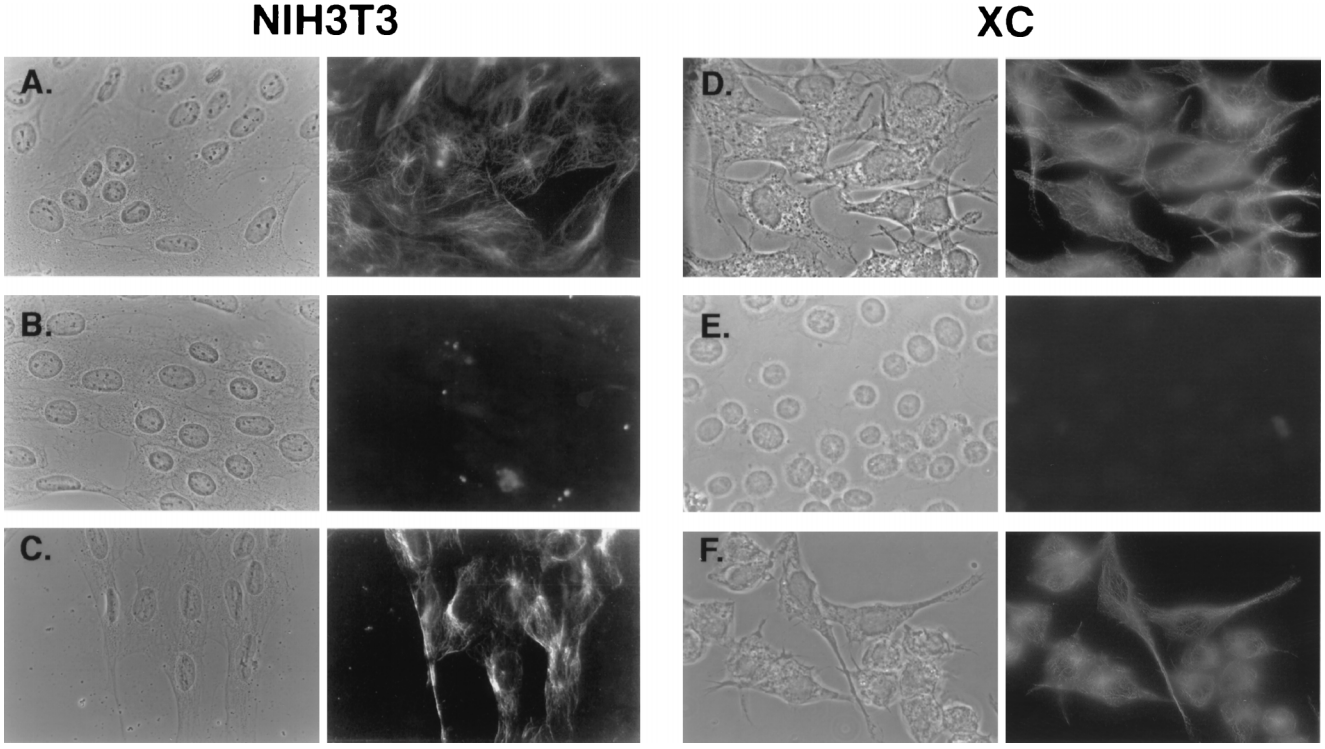

FIG. 3. Recovery of microtubule network organization occurs within 2 h after withdrawal of nocodazole treatment. Indirect immunofluorescence using a monoclonal antibody against β-tubulin was performed on NIH 3T3 and XC cells. (A and D) Untreated cells; (B and E) cells exposed to 66 μM nocodazole for 3 h; (C and F) cells exposed to 66 μM nocodazole for 3 h then allowed to recover for 2 h after removal of nocodazole. The left panel of each section shows the phase-contrast photomicrograph of the cells viewed by fluorescence microscopy in the right panel.

particularly in the NIH 3T3 cultures. If so, then the decrease in infection of NIH 3T3 cells might not be due to a requirement for microtubules in virus entry. Again we determined the number of cell divisions from the increase in cell density upon termination of each experiment. If the 3-h exposure to nocodazole imposed a block to the cell cycle that remained after the drug's removal, then the number of cell divisions in the untreated cultures would be much greater than that in the treated

TABLE 3. Infection in nocodazole-treated cells

Cell line	Expt[a]	% Infected cells[b]		Relative infection[c] (%)	Relative inhibition[d] (%)	Avg
		No inhibitor	Nocodazole			
NIH 3T3	Pre					
	33 μM I	0.390 ± 0.055	0.099 ± 0.017	25	75	
	II	0.390 ± 0.011	0.170 ± 0.015	44	56	71
	III	0.510 ± 0.015	0.093 ± 0.009	18	82	
	66 μM IV	0.340 ± 0.030	0.046 ± 0.004	14	86	NA[e]
	Post					
	I	0.056 ± 0.010	0.012 ± 0.002	21	79	
	II	0.073 ± 0.005	0.014 ± 0.002	19	81	81
	III	0.063 ± 0.017	0.010 ± 0.002	16	84	
XC	Pre					
	33 μM I	0.129 ± 0.019	0.108 ± 0.012	84	16	
	II	0.186 ± 0.016	0.175 ± 0.030	94	6	7
	III	0.130 ± 0.004	0.130 ± 0.010	100	0	
	66 μM IV	0.580 ± 0.020	0.590 ± 0.013	102	↑ 2	NA
	Post					
	I	0.060 ± 0.005	0.056 ± 0.010	93	7	
	II	0.224 ± 0.017	0.187 ± 0.005	83	17	2
	III	0.093 ± 0.008	0.110 ± 0.004	118	↑ 18	

[a] Pre, pretreatment. Cells were exposed to either 33 or 66 μM nocodazole for 45 min and then exposed to the inhibitor plus ecotropic virus for an additional 2 h as described in Materials and Methods. Post, postinternalization. Nocodazole at 66 μM was added to cells 20 min after virus internalization.
[b] (Number of infected cells/total number of cells) × 100. Values shown are the mean of replicate samples ± 1 standard deviation ($n = 4$).
[c] (Percent infected cells in the treated population/percent infected cells in the untreated population) × 100.
[d] Calculated as (100 − relative infection). Values representing an increase in infection are indicated by arrows.
[e] NA, not applicable.

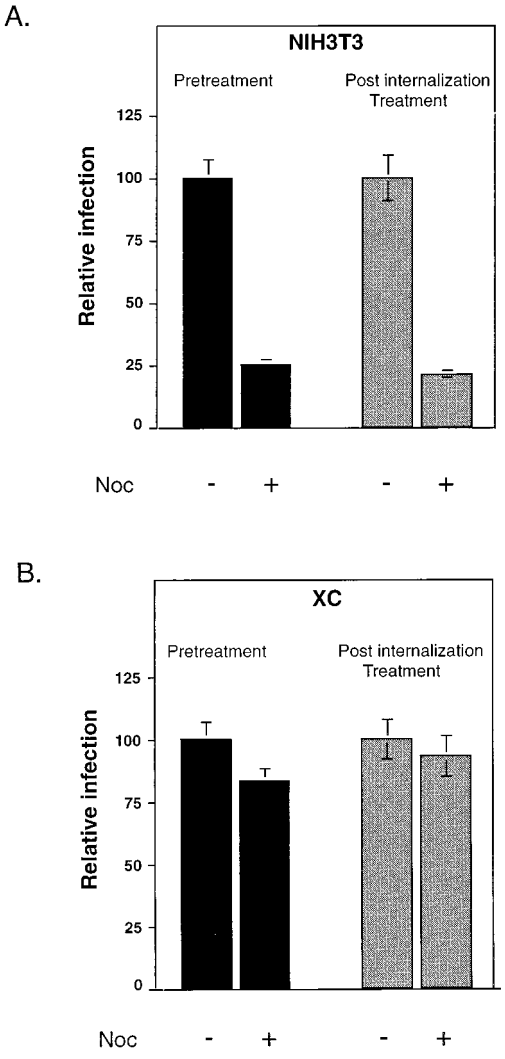

FIG. 4. Depolymerization of the microtubule network reduces ecotropic virus infection in NIH 3T3 cells by affecting an event after internalization of virus. Pretreatment, cells were treated for 45 min with 33 μM nocodazole (Noc) and then incubated with ψ-2 BAG virus for 2 h in the presence of the drug. Postinternalization Treatment, cells were treated with 66 μM nocodazole 20 min after virus internalization as described in Materials and Methods. Values shown are infection data from postinternalization experiment I for both cell lines and are the means of four samples for each treatment. The error bars represent maximal variation.

cultures. Untreated NIH 3T3 cultures averaged 3.2 divisions, compared to 2.9 divisions in cultures pretreated with nocodazole (Table 2). Because the untreated cultures were infected (Table 3), they must have undergone at least one of the three divisions after they were exposed to virus (41). Since the treated cultures underwent a comparable number of divisions as untreated cells, they most likely underwent at least one mitosis after exposure to the virus and inhibitors as well. Infection of XC cells exposed to nocodazole was only slightly less than that in untreated cultures (Table 3) even though treated cultures averaged 3.1 cell divisions, compared to 3.6 divisions in untreated cells (Table 2). These data suggest that a difference of as great as one-half division is not sufficient decrease in mitosis to account for a marked decrease in infection. Thus, it is unlikely that the average 0.3 cell division difference seen in NIH 3T3 cultures could represent a block in the cell cycle that interfered with virus infection sufficiently to account for the marked decrease in infection observed.

The inhibition of infection was not profoundly affected by MOI. In pretreatment experiments, we had exposed cells to virus at multiplicities of infection (MOIs) of approximately 0.1 for 2 h. We then examined infection in inhibitor-treated cells, using MOIs of 0.01 and 1 to determine if increasing or decreasing the virus concentration would alter the effects of the inhibitors on virus infection. The inhibition of infection in cytochalasin D-treated NIH 3T3 and XC cells remained approximately the same as virus was increased, suggesting that the concentration of available virus was not a factor in the observed effects. Similarly, infection of XC cells treated with nocodazole was insensitive to the saturation of the system. However, increasing the amount of available virus somewhat relieved the inhibition to infection caused by nocodazole treatment in NIH 3T3 cells. Infection was decreased by 79% at an MOI of 0.01, 74% at an MOI of 0.1, and 61% at an MOI of 1 (Fig. 5).

The depolymerization of the microtubules and actin network does not down-regulate the surface expression of the virus receptor. Given the gross morphological changes in treated cells, it was possible that the surface expression of the virus receptor was down-regulated by these cytoskeletal inhibitors. If this were the case, any observed effect of infection would be attributable to a lack of virus binding sites rather than to an involvement of cytoskeletal components in entry. Taking advantage of the cellular function of the receptor as the principal cationic amino acid transporter (22, 52), we measured L-arginine uptake in treated cells and compared it to uptake in untreated cells to evaluate surface expression.

Figure 6 shows the mean values of L-arginine transport in NIH 3T3 and in XC cells after 45 min, 2 h, and 3 h of exposure to the inhibitors. Transport was comparable in untreated, DMSO-treated, and nocodazole- or cytochalasin D-treated cells of both cell types, suggesting that the receptor remains on the cell surface upon treatment with these drugs. After a 3-h treatment with cytochalasin D, NIH 3T3 cells transported a mean of 1% more L-arginine than was transported by untreated cells (Fig. 6A), and XC cells transported a mean of 1% less L-arginine than did untreated cells (Fig. 6B). After a 3-h treatment with 66 μM nocodazole, NIH 3T3 cells transported a mean of 7% less L-arginine than did untreated cells (Fig. 6C) and XC cells transported a mean of 1% less L-arginine than did untreated cells (Fig. 6D). Because the cytoskeletal inhibitors nocodazole and cytochalasin D were dissolved in DMSO prior to application on to cells, cells treated only with DMSO were included in all experiments to measure any effects due to the presence of DMSO. Transport in cells treated with DMSO alone was also comparable to that in untreated cells (data not shown).

In addition, we measured the transport of another cationic amino acid substrate for the receptor, L-lysine, in three independent experiments after a 45-min exposure to the inhibitors. The results were in agreement with those found for L-arginine transport. After cytochalasin D treatment, NIH 3T3 cells transported a mean of 4% more and XC cells transported a mean of 7% more L-lysine than did untreated cells. L-Lysine transport was a mean of 15% less in NIH 3T3 cells and 1% greater in XC cells treated with 33 μM nocodazole than in untreated cells. Treatment with DMSO alone resulted in a mean decrease of 3% in NIH 3T3 cells and a mean increase of 8% in XC cells of L-lysine transport compared to untreated cells. These results also demonstrate that disruption of either the microtubules or actin network does not affect the physiological function of the transporter/receptor.

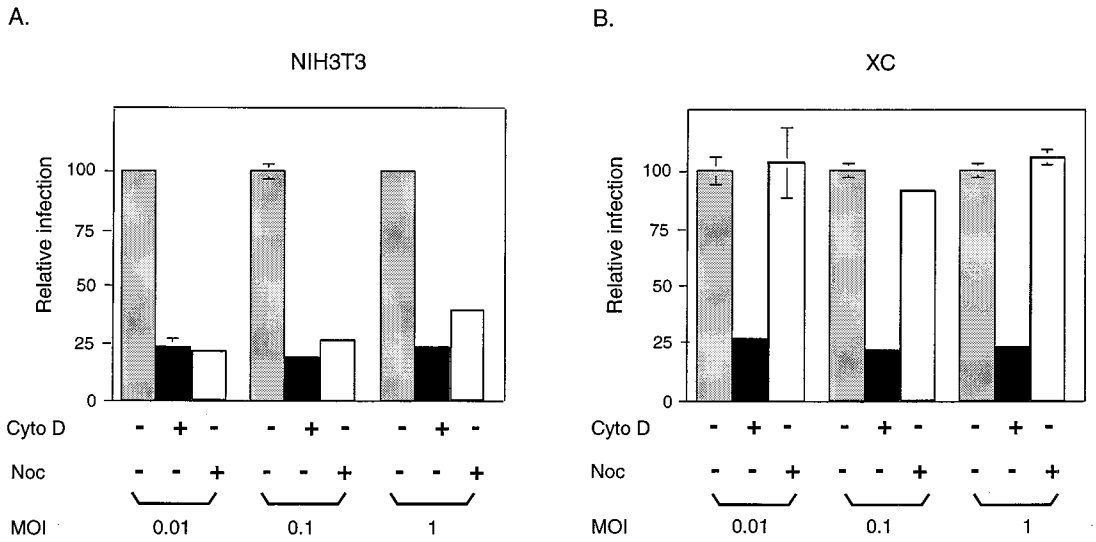

FIG. 5. The reduction in ecotropic virus infection resulting from the depolymerization of the actin network is independent of the MOI in NIH 3T3 and XC cells, but the inhibition of infection upon depolymerization of the microtubules is partially relieved in NIH 3T3 cells by increasing the MOI. The results shown are the means of four samples for each treatment. The error bars represent maximal variation. NIH 3T3 or XC cells were treated for 45 min with the indicated drug and then exposed to ψ-2 BAG virus at an MOI of 0.01, 0.1, or 1 for 2 h. The appropriate concentration of drug was maintained during virus exposure. Shaded bars, untreated cells; solid bars, cells treated with 1 μg of cytochalasin (Cyto) D per ml; open bars, cells treated with 33 μM nocodazole (Noc). When exposed to MOIs of 1, 0.1, and 0.01 for 2 h, 2.75% ± 0.10%, 0.28% ± 0.02%, and 0.03% ± 0.00%, respectively, of untreated NIH 3T3 cells were infected and 2.03% ± 0.11%, 0.22% ± 0.02%, and 0.024% ± 0.00%, respectively, of untreated XC cells were infected.

DISCUSSION

Inhibition of infection in NIH 3T3 and XC cells was similar to that reported in studies of the effects of cytochalasin D and nocodazole on the function of other membrane proteins: 70 to 75% inhibition of biological activity (11, 26, 34, 36, 42, 54). It is thought that the lack of complete inhibition in these studies was due to resistance to the action of the inhibitors. For example, sensitivity to cytochalasin D has been shown to depend on the stage of the cell cycle; that is, cells in G_1 are most sensitive, while cells in the S phase through G_2 are relatively insensitive (29). The lack of complete inhibition by nocodazole might be due to the presence of microtubules composed of Glu-tubulin, a minor variant of α-tubulin that is nocodazole resistant (21, 49). Alternatively, it is possible that the ecotropic receptor can mediate virus entry in cells that lack a complete cytoskeleton but functions more efficiently when the host cytoskeleton is intact. A third possibility is that there is more than one population of virus receptors on host cells: a predominant population whose activity is dependent on the cytoskeleton and a smaller population that is independent of the cytoskeleton. Some of the residual infection might be due to the 1% of bound but not internalized virus that resist inactivation by the low-pH citrate wash. However, this contribution is unlikely to account for most of the residual 20 to 30% infection.

The ecotropic virus receptor is an integral membrane protein (1) that functions as a cationic amino acid transporter in the host cell (22, 52). To address the possibility that depolymerization of the cytoskeleton might down-regulate the receptor, we used amino acid transport to evaluate surface expression. Amino acid transport was not decreased in NIH 3T3 cells after up to 3 h of exposure to 1 μg of cytochalasin D per ml or 66 μM nocodazole, suggesting that transporters remain on the surface. However, because a slight reduction of transporters (less than 10%) on the cell surface would not be detectable in the amino acid transport assay, we cannot rule out the possibility that only a small fraction of transporters are competent virus receptors and that these molecules were preferentially internalized upon drug treatment. Indeed, Wang et al. have suggested that only a small number of virus receptors on any cell are functional (53).

In experiments in which a profound inhibition of infection was not observed, there was frequently a slight decrease in infection. For example, NIH 3T3 cells exposed to cytochalasin D after virus internalization exhibited an average 2% decrease in infection compared to untreated cells. Nocodazole exposure before and after virus internalization resulted in 7 and 2% average decreases in infection of XC cells. It is difficult to interpret the relevance of such small but consistent decreases. In particular, the relevance of the 16 and 6% decreases in infection observed in XC cells pretreated with 33 μM nocodazole are difficult to interpret in light of the third experiment, where no decrease was observed, and the experiment with 66 μM nocodazole, in which a 2% increase in infection was observed. The small decreases in cell division observed in most of the experiments might reflect a low level of blocked cell division that was responsible for the slight decrease in infection. However, there was no consistent correlation between a slight reduction in infection and a decrease in cell division. For example, the largest such reduction (16%) was observed for XC cultures in which both untreated and treated cells averaged 3.2 divisions, and the second largest difference in division (3.8 versus 2.4) was observed in the XC cells, for which there was a 13% increase in infection in treated cultures.

One possible explanation for the lack of inhibition of infection in XC cells exposed to nocodazole might be that XC cells are more resistant to the inhibitor's effects than NIH 3T3 cells. If XC cells were more resistant, then their microtubules might not be depolymerized to an extent that would decrease virus infection as markedly as in NIH 3T3 cultures, masking an involvement of microtubules in infection of XC cells. However, the microtubules in XC cells had depolymerized by the end of a 3-h exposure and repolymerized within 2 h after removal of

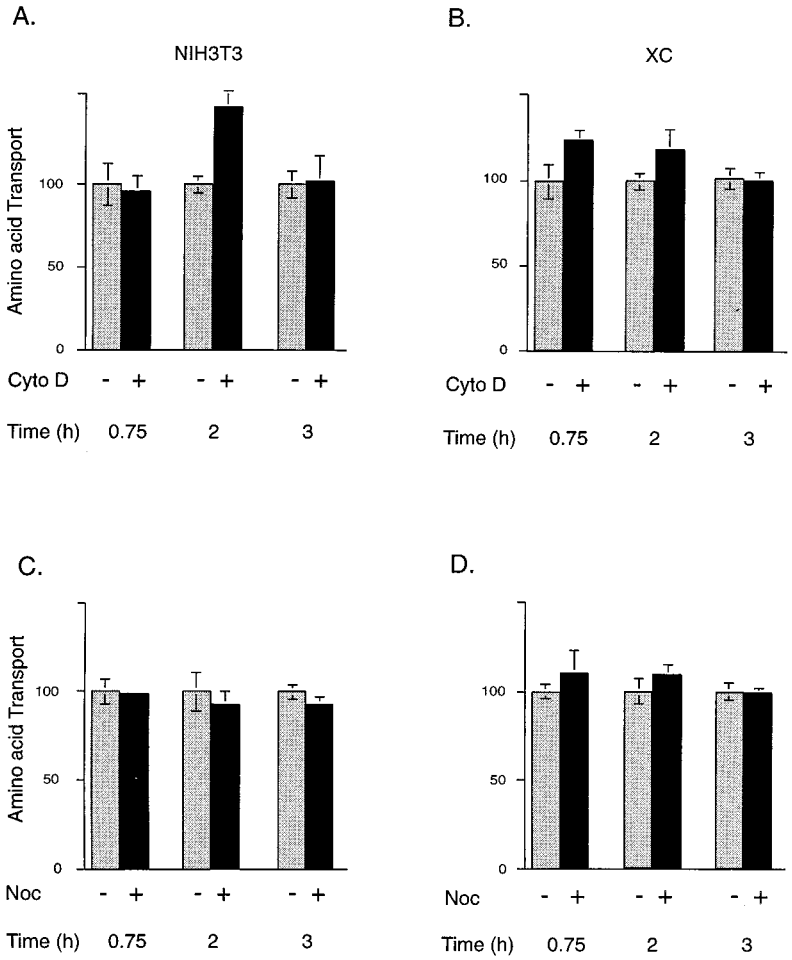

FIG. 6. Disruption of the microtubule and the actin network does not affect the uptake of cationic amino acids mediated by the virus receptor in NIH 3T3 and XC cells. Cationic amino acid uptake assays were performed on NIH 3T3 and XC cells after treatment with 1 μg of cytochalasin (Cyto) D per ml (upper panels) or 66 μM nocodazole (Noc) (lower panels) for the times indicated. The appropriate treatments were maintained during the uptake assay. Values shown in the graph are L-arginine transport relative to that of untreated cells in the same experiment, calculated from the mean nanomoles of L-arginine transported/minute/milligram of protein ($n = 4$).

the inhibitor, just as the microtubules in NIH 3T3 cultures had. We cannot exclude the possibility that there are subtle differences in sensitivity to nocodazole between XC and NIH 3T3 cells.

Models for ecotropic virus entry. The question remains unanswered as to why the site of ecotropic virus fusion differs with the host cell. Because only infection of rat XC cells appears to occur by cell surface fusion, the site of virus fusion might correlate with differences between the mouse and rat receptors. Recent isolation of the rat homolog of the receptor revealed that there are four divergent residues and a three-amino-acid insertion in the virus binding site of the rat sequence, although the two proteins are 97% identical (35, 58). However, these differences are unlikely to explain the observations because infection of normal rat kidney and Rat-1 cells appears to occur via the endocytic pathway (28).

Other studies have shown that ecotropic viruses induce cell-cell fusion of XC cells at neutral pH (23, 59) but do not induce extensive fusion of NIH 3T3 fibroblasts, L8 myoblasts, and Rat-1 cells. Transformation of NIH 3T3 cells with the *ras* oncogene or of L8 and Rat-1 cells with Rous sarcoma virus bearing the *src* oncogene rendered them capable of extensive fusion in the presence of ecotropic virus (20, 56). Kaufman and Ehrbar (20) and Wilson et al. (56) suggested that changes in the cells upon transformation make them competent for cell surface fusion. Others demonstrated that transformation by *ras* or *src* alters the morphology of cells via changes in the organization of the microtubules and actin network (2, 6, 16, 18). Thus, the site of virus fusion might depend partly on the status of cytoskeletal components in the host cell. However, virus entry into the *ras*-transformed NIH 3T3 cells was still sensitive to lysosomal inhibitors, suggesting that the site of virus fusion did not change to the cell surface upon transformation, even though the cells were now very competent for cell-cell fusion.

We propose a simple model of ecotropic virus entry in which binding occurs via the same interactions between the virus and the receptor in all host cells, but that postbinding events, particularly virus internalization (plasma membrane penetration), differ between XC and other cells. Our data indicate that the actin network plays a critical role in an event prior to virus internalization that is common to entry into both NIH 3T3 and XC cells. Virus attachment would be a likely step that requires the critical contribution of the actin network. For instance, the actin network might exert a crucial influence that maintains a higher-order structure of the receptor essential to virus binding. It is also possible that the actin network does not influence virus binding; instead, virus binding might transmit a signal via the actin network that triggers a critical change in the host cell.

A sensitive assay for detecting subtle changes in receptor structure, combined with virus binding and fusion assays, should shed light on whether disruption of the actin network affects the attachment of the virus.

These studies suggest that intact microtubules are required in a postinternalization step for efficient infection of NIH 3T3 cells. They do not rule out the possibility that intact microtubules are also involved in an event prior to virus internalization. Our data imply that newly internalized virus particles are relatively unstable because virus infection was not efficiently salvaged when nocodazole was removed after the 3-h exposure in the postinternalization studies, even though the microtubules reorganized and cell division continued. In contrast, viral nucleoprotein complexes have been found to be very stable by 6 h after virus internalization (41). Roe et al. (41) exposed host cells to ecotropic virus and then 9 h later added nocodazole. They found that integration was blocked by the inhibitor but that the viral complexes remained integration competent when the drug was removed 10 h later. Conformational changes in the structural proteins, particularly the envelope proteins, are thought to occur upon binding and internalization. Perhaps further conformational changes are induced by uncoating during fusion, stabilizing the viral integration complex. Microtubules have been implicated in the movement of endocytic vesicles from the cell surface to the lysosomes (9). For example, during endocytosis of the transferrin receptor, vesicles containing the receptor are transported by a microtubule-dependent mechanism (19, 45). Perhaps in NIH 3T3 cells, disruption of the microtubules within 20 min of virus internalization blocks progression of virus-containing vesicles to the endosomal compartments where fusion presumably occurs. The prolonged stay in a compartment where fusion cannot occur might then target particles for degradation. If this were the case, then nocodazole would not be expected to affect infection in XC cells, where fusion, occurring presumably at the cell surface, would result in internalized viral complexes that have already been stabilized by changes during uncoating.

Andersen and coworkers reported that the virus surface protein SU is cleaved upon virus entry and that ecotropic virus-induced cell fusion is enhanced by exogenous proteinase treatment (3–5). McClure and colleagues postulated that the proteinase that cleaves SU may depend on the low pH of the endosome in NIH 3T3 cells but may function at neutral pH on the surface of XC cells, activating the fusion capability of SU at the cell surface (28). If this were the case, then internalization of ecotropic viruses would constitute a variation of the endocytic pathway in which fusion with cell membranes is triggered by protease digestion instead of exposure to low pH. Our data are consistent with this model. In this case, exposure to nocodazole might block movement of vesicles containing newly internalized virus to a compartment where the protease resides, thereby preventing virus fusion.

The physiological function of the receptor does not require an intact cytoskeleton. Recent studies have shown that the receptor and the homologous human and porcine amino acid transporters cluster on the surface of rat, human, and porcine cells, respectively (57). Looking specifically at human cells, Woodard and coworkers (57) found that the disruption of microtubules with nocodazole abolished this clustering, suggesting a possible interaction of the transporter/receptor with the cellular cytoskeleton. Studies of other plasma membrane proteins have revealed that the γ-aminobutyric acid receptor, the glycine receptor, and CD2 on T-cell surfaces interact with microtubules, while the *N*-methyl-D-aspartate receptor, neuronal voltage-gated sodium channels, and immunoglobulin G Fc receptor subclass I interact with actin (11, 13, 17, 26, 32–34). In each case, the interaction was shown to be critical for biological function (11, 26, 34, 36, 42, 54). However, our studies indicate that any interaction that the ecotropic receptor might have with either the actin network or the microtubules is not required for its function as the principal transporter of cationic amino acids in cells.

ACKNOWLEDGMENTS

We thank John Cox, Linda Hendershot, Jianxun Li, Shreenath Sharma, and Michael Whitt for many helpful discussions; John Cox and Jianxun Li for the rabbit antitubulin; and Michael Dockter for assistance with fluorescence microscopy. We thank David Armbruster for critical reading of the manuscript. We also thank Terrance Cooper for encouraging talks.

This work was funded by National Institutes of Health grant AI 33410 to L.M.A.

REFERENCES

1. **Albritton, L. M., L. Tseng, D. Scadden, and J. M. Cunningham.** 1989. A putative murine ecotropic retrovirus receptor gene encodes a multiple membrane-spanning protein and confers susceptibility to virus infection. Cell **57:**659–666.
2. **Anand, B., and I. N. Chou.** 1993. Microtubule network and microtubule-associated proteins in leukemic T-cells. Leukemia. **7:**51–57.
3. **Andersen, K. B.** 1987. Cleavage fragments of retrovirus protein during virus entry. J. Virol. **68:**2193–2202.
4. **Andersen, K. B.** 1985. Fate of the surface protein gp70 during entry of retrovirus into mouse fibroblasts. Virology **142:**112–120.
5. **Andersen, K. B., and H. Skov.** 1989. Retrovirus induced cell fusion is enhanced by protease treatment. J. Gen. Virol. **70:**1921–1927.
6. **Bhattcharya, B., F. Ciardiello, D. S. Salomon, and H. L. Cooper.** 1988. Disordered metabolism of microfilament proteins, tropomyosin and actin, in mouse mammary epithelial cells expressing the Ha-ras oncogene. Oncogene Res. **3:**51–65.
7. **Brinkley, B. R., S. H. Fistel, J. M. Marcum, and R. L. Pardue.** 1980. Microtubules in cultured cells; indirect immunofluorescence staining with tubulin antibody. Int. Rev. Cytol. **63:**59–95.
8. **Charlton, C. A., and L. E. Volkman.** 1993. Penetration of *Autographa california* nuclear polyhedrosis virus nucleocapsid into IPLB Sf 21 cells induce actin cable formation. Virology **197:**245–254.
9. **Cole, N. B., and J. Lippincott-Schwartz.** 1995. Organization of organelles and membrane traffic by microtubules. Curr. Opin. Cell Biol. **7:**55–64.
10. **De Brabander, M. J., R. M. L. Van deVeire, F. E. M. Aerts, M. Borgers, and P. A. Janssen.** 1976. The effects of methyl[5-(2-thienylcarbonyl)-1H-benzimidazole-2yl] carbamate (R 17934;NSC 238159), a new synthetic antitumoral drug interfering with microtubules, on mammalian cells cultured in vitro. Cancer Res. **36:**905–916.
11. **Froehner, S. C.** 1993. Regulation of ion channel distribution at synapses. Annu. Rev. Neurosci. **16:**347–368.
12. **Gail, M. H., and C. W. Boone.** 1971. Cytochalasin effects on BALB/3T3 fibroblasts: dose dependent, reversible alteration of motility and cytoplasmic cleavage. Exp. Cell Res. **68:**226–228.
13. **Geppert, T. D., and P. E. Lipsky.** 1991. Association of various T-cell surface molecules with the cytoskeleton. Effect of cross-linking and activation. J. Immunol. **146:**3298–3305.
14. **Gilbert, J. M., D. Mason, and J. M. White.** 1990. Fusion of Rous sarcoma virus with host cells does not require exposure to low pH. J. Virol. **64:**5106–5113.
15. **Hamilton, B. T., and J. A. Snyder.** 1982. Rapid completion of mitosis and cytokinesis in PtK_1 cells following release from nocodazole arrest. Eur. J. Cell Biol. **28:**190–194.
16. **Hansell, E. J., S. M. Frisch, P. Tremble, J. P. Murnane, and Z. Werb.** 1995. Simian virus 40 transformation alters the actin cytoskeleton, expression of metalloproteinases and invasive behaviour of normal and ataxia-telangiectasia human skin fibroblast. Biochem. Cell Biol. **73:**373–389.
17. **Item, C., and W. Sieghart.** 1994. Binding of γ-aminobutyric acid receptor to tubulin. J. Neurochem. **63:**1119–1125.
18. **Janmey, P. A., and C. Chaponnier.** 1995. Medical aspects of the actin cytoskeleton. Curr. Opin. Cell Biol. **7:**111–117.
19. **Jin, M., and M. D. Snyder.** 1993. Role of microtubules in transferrin receptor transport from the cell surface to the endosomes and the Golgi complex. J. Biol. Chem. **268:**18390–18397.
20. **Kaufman, S. J., and D. M. Ehrbar.** 1980. Transformation of rat fibroblasts and formation of virus-induced syncytia. Nature **285:**484–485.
21. **Khawaja, S., G. G. Gundersen, and J. C. Bulinski.** 1988. Enhanced stability of microtubules enriched in detyrosinated tubulin is not a direct function of detyrosination level. J. Cell Biol. **106:**141–149.
22. **Kim, J. W., E. I. Closs, L. M. Albritton, and J. M. Cunningham.** 1991.

Transport of cationic amino acids by the mouse ecotropic retrovirus receptor. Nature **352:**725–728.
23. **Klement, V., W. P. Rowe, J. W. Hartley, and W. E. Pugh.** 1969. Mixed culture cytopathogenicity: a new test for growth of murine leukemia viruses in tissue culture. Proc. Natl. Acad. Sci. USA **63:**753–758.
24. **Kreutz, L. C., and M. R. Ackermann.** 1996. Porcine reproductive and respiratory syndrome virus enters cells through a low pH-dependent endocytic pathway. Virus Res. **42:**137–147.
25. **Maddon, P. J., J. S. McDougal, P. R. Clapham, A. G. Dalgleish, S. Jamal, R. A. Weiss, and R. Axel.** 1988. HIV infection does not require endocytosis of its receptor, CD4. Cell **54:**865–874.
26. **Mattson, M. P., H. Wang, and E. K. Michaelis.** 1991. Developmental expression, compartmentalization, and possible role in excitotoxicity of a putative NMDA receptor protein in cultured hippocampal neurons. Brain Res. **565:**94–108.
27. **McClure, M. O., M. Marsh, and R. A. Weiss.** 1988. Human immunodeficiency virus infection of CD4-bearing cells occurs by a pH-independent mechanism. EMBO J. **7:**513–518.
28. **McClure, M. O., M. A. Sommerfelt, M. Marsh, and R. A. Weiss.** 1990. The pH independence of mammalian retrovirus infection. J. Gen. Virol. **71:**767–773.
29. **Miranda, A. F., G. C. Godman, A. D. Deitch, and S. W. Tanenbaum.** 1974. Action of cytochalasin D on cells of established lines. I. Early events. J. Cell Biol. **61:**481–500.
30. **Miranda, A. F., G. C. Godman, and S. W. Tanenbaum.** 1974. Action of cytochalasin D on cells of established lines. II. Cortex and microfilaments. J. Cell Biol. **62:**406–423.
31. **Miyamoto, K., and R. V. Gilden.** 1971. Electron microscopic studies of tumour viruses. I. Entry of murine leukemia viruses into mouse embryo fibroblasts. J. Virol. **7:**395–405.
32. **Neithammer, M., E. Kim, and M. Sheng.** 1996. Interaction between the C terminus of NMDA receptor subunits and multiple members of the PSD-95 family of membrane-associated guanylate kinases. J. Neurosci. **16:**2157–2163.
33. **Offringa, R., and B. E. Bierer.** 1993. Association of CD2 with tubulin. J. Biol. Chem. **268:**4979–4988.
34. **Ohta, Y., T. P. Stossel, and J. H. Hartwig.** 1991. Ligand-sensitive binding of actin-binding protein to immunoglobulin G Fc receptor I (FcγRI). Cell **67:**275–282.
35. **Puppi, M., and S. J. Henning.** 1995. Cloning of the rat ecotropic retroviral receptor and studies of its expression in intestinal tissues. Proc. Soc. Exp. Biol. Med. **209:**38–45.
36. **Rabinowich, H., W. C. Lin, R. B. Herberman, and T. L. Whiteside.** 1994. Signaling via CD7 molecules on human NK cells. Induction of tyrosine phosphorylation and β 1 integrin mediated adhesion to fibronectin. J. Immunol. **153:**3504–3513.
37. **Redmond, S., G. Peters, and C. Dickson.** 1984. Mouse mammary tumor virus can mediate cell fusion at reduced pH. Virology **133:**393–402.
38. **Rein, A., and R. H. Bassin.** 1978. Replication-defective ecotropic murine leukemia viruses: detection and quantitation of infectivity using helper-dependent XC plaque formation. J. Virol. **28:**656–660.
39. **Rein, A., B. I. Gerwin, R. H. Bassin, L. Schwarm, and G. Schidlovsky.** 1978. A replication-defective variant of Moloney murine leukemia virus. I. Biological characterization. J. Virol. **25:**146–156.
40. **Risco, C., L. Menedez-Arias, T. D. Copeland, P. Pinto da Silva, and S. Oroszlan.** 1995. Intracellular transport of the murine leukemia virus during acute infection of NIH3T3 cells: nuclear import of nucleocapsid protein and integrase. J. Cell Sci. **108:**3039–3050.
41. **Roe, T. Y., T. C. Reynolds, G. Yu, and P. O. Brown.** 1993. Integration of murine leukemia virus depends on mitosis. EMBO J. **12:**2099–2108.
42. **Rosenmund, C., and G. L. Westbrook.** 1993. Calcium-induced actin depolymerization reduces NMDA channel activity. Neuron **10:**805–814.
43. **Rosenthal, K. S., M. B. Leuther, and B. G. Barisas.** 1984. Herpes simplex virus binding and entry modulates cell surface protein mobility. J. Virol. **49:**980–983.
44. **Rosenthal, K. S., R. Perez, and C. Hodnichak.** 1985. Inhibition of herpes simplex virus type I penetration by cytochalasins B and D. J. Gen. Virol. **66:**1601–1605.
45. **Sakai, S., S. Yamashina, and S. Ohnishi.** 1991. Microtubule-disrupting drugs blocked delivery of endocytosed transferrin to the cytocenter, but did not affect return of transferrin to plasma membrane. J. Biochem. **109:**528–533.
46. **Schroeder, T. E.** 1970. The contractile ring I: fine structure of dividing mammalian (HeLa) cells and effects of cytochalasin B. Zellforsch. Mikrosk. Anat. **109:**431–449.
47. **Shimura, H., Y. Umeno, and G. Kimura.** 1987. Effects of inhibitors of the cytoplasmic structures and functions on the early phase of infection of cultured cells with simian virus 40. Virology **158:**34–43.
48. **Stein, B. S., S. D. Gowda, J. D. Lifson, R. C. Penhallow, K. G. Bensch, and E. G. Engleman.** 1987. pH-independent HIV entry into CD4-positive T cells via virus envelope fusion to the plasma membrane. Cell **49:**659–668.
49. **Thyberg, J., and S. Moskalewski.** 1989. Subpopulation of microtubules with differential sensitivity to nocodazole: role in the structural organization of the Golgi complex and the lysosomal system. J. Submicrosc. Cytol. Pathol. **21:**259–274.
50. **Turner, D. L., and C. L. Cepko.** 1987. A common progenitor for neuron and glia persists in rat retina late in development. Nature **328:**131–136.
51. **Wang, H., E. Dechant, M. Kavanaugh, R. A. North, and D. Kabat.** 1994. Effects of ecotropic murine retroviruses on the dual function cell surface receptor/basic amino acid transporter. J. Biol. Chem. **267:**23617–23624.
52. **Wang, H., M. P. Kavanaugh, R. A. North, and D. Kabat.** 1991. Cell-surface receptor for ecotropic murine retroviruses is a basic amino-acid transporter. Nature **352:**719–731.
53. **Wang, H., R. Paul, R. E. Burgeson, D. R. Keene, and D. Kabat.** 1991. Plasma membrane receptors for ecotropic murine retroviruses require a limiting accessory factor. J. Virol. **65:**6468–6477.
54. **Whatley, V. J., S. J. Mihic, A. M. Allan, S. J. McQuillkin, and R. A. Harris.** 1994. γ-Aminobutyric acid receptor function is inhibited by microtubule depolymerization. J. Biol. Chem. **269:**19546–19552.
55. **White, J., K. Matlin, and A. Helenius.** 1981. Cell fusion by Semliki forest, influenza, and vesicular stomatitis viruses. J. Cell Biol. **89:**674–679.
56. **Wilson, C. A., J. W. Marsh, and M. V. Eiden.** 1992. The requirements of viral entry differ from those for virally induced syncytium formation in NIH 3T3/DTras cells exposed to Moloney murine leukemia virus. J. Virol. **66:**7262–7269.
57. **Woodard, M. H., W. A. Dunn, R. O. Laine, M. Malandro, R. McMahon, O. Simell, E. R. Block, and M. S. Kilberg.** 1994. Plasma membrane clustering of the system y+ (CAT-1) amino acid transporter as detected by immunohistochemistry. Am. J. Physiol. **266:**E817–E824.
58. **Wu, J. Y., D. Robinson, H. J. Kung, and M. Hatzaglou.** 1994. Hormonal regulation of the gene for the type C ecotropic retrovirus receptor in rat liver cell. J. Virol. **68:**1615–1623.
59. **Zarling, D. A., and I. Keshet.** 1979. Fusion activity of virions of murine leukemia virus. Virology **95:**185–196.
60. **Zhai, Y., and G. G. Borisy.** 1994. Quantitative determination of microtubule polymer present during the mitosis-interphase transition. J. Cell Sci. **107:**881–890.
61. **Zieve, G. W., D. Turnbull, M. Mullins, and J. R. McIntosh.** 1980. Production of large numbers of mitotic mammalian cells by use of the reversible microtubule inhibitor nocodazole. Exp. Cell Res. **126:**397–405.